Article

Not peer-reviewed version

Antitumor Activities of Chimeric Anti-EphA2 Antibodies in Xenograft Models of Breast, Pancreatic, and Colorectal Cancers

Guanjie Li , Hiroyuki Suzuki , Tomokazu Ohishi , Hiroyuki Satofuka , Kenichiro Ishikawa , Kai Shimizu , Airi Nomura , Haruto Araki , Naoki Kojo , Kaito Suzuki , Saori Handa , Takuro Nakamura , Miyuki Yanaka , Tomohiro Tanaka , Mika K. Kato , Yukinari Kato *

Posted Date: 9 December 2025

doi: 10.20944/preprints202512.0860.v1

Keywords: monoclonal antibody therapy; EphA2; ADCC; CDC; breast cancer; pancreatic cancer; colorectal cancer

 doi:10.20944/preprints202512.0860.v1

Article

Antitumor Activities of Chimeric anti-EphA2 Antibodies in Xenograft Models of Breast, Pancreatic, and Colorectal Cancers

Guanjie Li [1], Hiroyuki Suzuki [1], Tomokazu Ohishi [2], Hiroyuki Satofuka [1], Kenichiro Ishikawa [1], Kai Shimizu [1], Airi Nomura [1], Haruto Araki [1], Naoki Kojo [1], Kaito Suzuki [1], Saori Handa [1], Takuro Nakamura [1], Miyuki Yanaka [1], Tomohiro Tanaka [1], Mika K. Kaneko [1] and Yukinari Kato [1,*]

[1] Department of Antibody Drug Development, Tohoku University Graduate School of Medicine, 2-1 Seiryo-machi, Aoba-ku, Sendai, Miyagi 980-8575, Japan

[2] Institute of Microbial Chemistry (BIKAKEN), Laboratory of Oncology, Microbial Chemistry Research Foundation, 3-14-23 Kamiosaki, Shinagawa-ku, Tokyo 141-0021, Japan

* Correspondence: yukinari.kato.e6@tohoku.ac.jp (Y.K.); Tel.: +81-22-717-8207 (Y.K.)

Abstract

Erythropoietin-producing hepatocellular receptor A2 (EphA2) has emerged as a key mediator that promotes tumor malignant progression. EphA2 overexpression and its non-canonical signaling lead to oncogenic transformation, metabolic reprogramming, resistance to treatments, and metastasis. Therefore, strategies targeting EphA2 have been evaluated in clinical trials. However, the clinical effects were not sufficient. An anti-EphA2 monoclonal antibody (mAb), Ea$_2$Mab-7 (mouse IgG$_1$, κ), demonstrated high affinity and specificity among Eph receptors. In this study, we produced recombinant class-switched Ea$_2$Mab-7 variants, including Ea$_2$Mab-7-mG$_{2a}$ (mouse IgG$_{2a}$) and Ea$_2$Mab-7-hG$_1$ (human IgG$_1$). Both Ea$_2$Mab-7-mG$_{2a}$ and Ea$_2$Mab-7-hG$_1$ recognized human triple-negative breast cancer MDA-MB-231, pancreatic cancer MIA PaCa-2, and colorectal cancer HCT-15 in flow cytometry. Furthermore, both Ea$_2$Mab-7-mG$_{2a}$ and Ea$_2$Mab-7-hG$_1$ exerted significant antibody-dependent cellular cytotoxicity and complement-dependent cytotoxicity against these tumors. In mouse xenograft models of breast, pancreatic, and colorectal cancers, both mAbs demonstrated antitumor activity. These results indicate the potential of Ea$_2$Mab-7 variants for the treatment of EphA2-positive cancers.

Keywords: monoclonal antibody therapy; EphA2; ADCC; CDC; breast cancer; pancreatic cancer; colorectal cancer

1. Introduction

The erythropoietin-producing hepatocellular (Eph) receptor family constitutes the largest subclass of receptor tyrosine kinases (RTKs) [1] and orchestrates essential physiological processes including embryonic patterning, axon guidance, synaptic formation, and vascular remodeling [2-4]. Eph receptors are also implicated in numerous pathological conditions, including cardiovascular diseases [5], disorders of the central nervous system [6], viral infections [7], and various tumors [1]. Among the 14 Eph receptors, EphA2 has been extensively studied in multiple solid tumors [1]. Notably, its functional role remains context-dependent and sometimes paradoxical, as EphA2 signaling can exert either pro-tumorigenic or anti-tumorigenic effects depending on ligand availability [8] and cellular or tumor-specific settings [9].

EphA2 binds to ephrin-A ligands, which facilitate intercellular communication between identical or distinct cell types through bidirectional signaling, forward and reverse signaling [4,10,11].

 doi:10.20944/preprints202512.0860.v1

This bidirectional signaling of the EphA2–ephrin-A complex is further amplified by the formation of higher-order oligomeric assemblies, referred to as receptor–ligand clustering [1]. The canonical EphA2 forward signaling is mediated by its RTK activity, which is linked to tumor-suppressing activities [3]. In contrast, non-canonical EphA2 signaling, which is independent of ligand engagement and RTK activity, is characterized by phosphorylation of S897 in the short segment of intracellular domain [8,12]. The S897 is phosphorylated by AKT [8], ribosomal S6 kinase [13], and protein kinase A families [14], which have been widely associated with tumor-promoting activities. EphA2 overexpression and the non-canonical signaling involving S897 phosphorylation lead to oncogenic transformation [15], metabolic reprogramming [16], resistance to treatments [17-19], and metastasis [20]. The EphA2 overexpression and/or the S897 phosphorylation are closely associated with poor clinical outcomes in breast cancer [21], pancreatic cancer [22], and colorectal cancer [23]. Therefore, EphA2 has emerged as a promising therapeutic target by various modalities, including monoclonal antibody (mAb) [1].

Several EphA2–targeting mAbs have been generated that either activate or inhibit forward signaling. They promote receptor internalization, elicit antibody-dependent cellular cytotoxicity (ADCC), or serve as delivery vehicles for antitumor agents and imaging probes to EphA2-positive tumors [1]. Among EphA2-directed mAbs showing preclinical efficacy are MM-310, an antagonistic antibody used to direct liposomes containing a docetaxel prodrug to tumor sites [24]; MEDI-547, an antibody–drug conjugate (ADC) linked to monomethyl auristatin F [25]; and DS-8895a, an afucosylated mAb to enhance ADCC [26]. However, clinical development of MM-310, MEDI-547, and DS-8895a was terminated due to unacceptable toxicities—bleeding and coagulation abnormalities and elevations in liver enzymes in MEDI-547 [27] and peripheral neuropathy known as a docetaxel-associated toxicity in MM-310 [1,28], and limited therapeutic efficacy in DS-8895a [29].

To target EphA2 receptors, our group has developed mAbs against EphA2 (Ea$_2$Mabs) using the Cell-Based Immunization and Screening (CBIS) method. Among 94 clones of Ea$_2$Mabs, an anti-EphA2 mAb (clone Ea$_2$Mab-7) detects EphA2-positive cells in flow cytometry, western blotting, and immunohistochemistry [30]. Therefore, Ea$_2$Mab-7 has potential for application in tumor therapy. In this study, we engineered Ea$_2$Mab-7 into a mouse IgG$_{2a}$-type (Ea$_2$Mab-7-mG$_{2a}$) and a human IgG$_1$-type (Ea$_2$Mab-7-hG$_1$) mAb and evaluated ADCC, complement-dependent cytotoxicity (CDC), and antitumor efficacy in EphA2-positive tumor xenograft models.

2. Materials and Methods

2.1. Cell Lines

The human pancreatic cancer cell line MIA PaCa-2, the colorectal cancer cell line HCT-15, and the human embryonic fibroblast cell line KMST-6 were obtained from the Cell Resource Center for Biomedical Research, Institute of Development, Aging and Cancer, Tohoku University (Miyagi, Japan). The human triple-negative breast cancer (TNBC) MDA-MB-231 cells were obtained from the American Type Culture Collection (Manassas, VA, USA). Human embryonic kidney 293FT was purchased from Thermo Fisher Scientific Inc. (Thermo, Waltham, MA, USA). A TERT-expressed normal cornea epithelial cell line, hTCEpi, was purchased from EVERCYTE (Vienna, Austria). Eph receptor overexpressed Chinese hamster ovary-K1 (e.g., CHO/EphA2) were previously established [31]. These cell lines were cultured as described previously [30,32].

2.2. Recombinant mAb Production

To generate recombinant mouse IgG$_{2a}$-type Ea$_2$Mab-7 (Ea$_2$Mab-7-mG$_{2a}$) and human IgG$_1$-type Ea$_2$Mab-7 (Ea$_2$Mab-7-hG$_1$), the V$_H$ and V$_L$ cDNAs of Ea$_2$Mab-7 (mouse IgG$_1$, κ) were cloned into pCAG-Neo and pCAG-Ble vectors (FUJIFILM Wako Pure Chemical Corporation, Osaka, Japan), together with the corresponding constant regions of mouse IgG$_{2a}$ [33] and human IgG$_1$ [34], respectively. Antibody expression vectors were transfected into ExpiCHO-S cells using the ExpiCHO Expression System to produce Ea$_2$Mab-7-mG$_{2a}$ and Ea$_2$Mab-7-hG$_1$. The PMab-231 (mouse IgG$_{2a}$) [33] and humCvMab-62 (human IgG$_1$) [34] were used as isotype control human IgG$_1$ (hIgG$_1$) and mouse IgG$_{2a}$ (mIgG$_{2a}$), respectively. All antibodies were purified using Ab-Capcher (ProteNova Co., Ltd.,

 doi:10.20944/preprints202512.0860.v1

Kagawa, Japan). These mAbs were denatured by SDS sample buffer (Nacalai Tesque, Inc., Kyoto, Japan) containing 2-mercaptoethanol and subject to SDS-PAGE. The gel was stained with Bio-Safe CBB G-250 Stain (Bio-Rad Laboratories, Inc., Berkeley, CA, USA).

2.3. Animals

The animal study for the antitumor efficacy of Ea$_2$Mab-7-mG$_{2a}$ and Ea$_2$Mab-7-hG$_1$ was approved by the Institutional Committee for Experiments of the Institute of Microbial Chemistry (Numazu, Japan, approval no. 2025-040) within which the work was undertaken and that it conforms to the provisions of the Declaration of Helsinki. Humane objectives for euthanasia were established as a loss of original body weight to a point >25% and/or a maximal tumor size >3,000 mm^3.

2.4. Flow Cytometry

Cells were harvested using 1 mM ethylenediaminetetraacetic acid (EDTA; Nacalai Tesque, Inc., Kyoto, Japan) in phosphate-buffered saline (PBS). The cells were treated with primary mAbs in blocking buffer (0.1% bovine serum albumin in PBS) for 30 min at 4°C. Then, the cells were treated with Alexa Fluor 488-conjugated anti-mouse IgG (1:2000; Cell Signaling Technology, Inc., Danvers, MA, USA) or fluorescein isothiocyanate (FITC)-conjugated anti-human IgG (1:2000; Sigma-Aldrich Corp., St. Louis, MO, USA for 30 minutes at 4°C. Fluorescence data were collected using the SA3800 Cell Analyzer (Sony Corp., Tokyo, Japan) and analyzed with FlowJo software (BD Biosciences, Franklin Lakes, NJ, USA).

2.5. ADCC

Five-week-old female BALB/c nude mice were purchased from Japan SLC, Inc. (Shizuoka, Japan). Effector cells were isolated from the spleens as described previously [35]. Target cells (MDA-MB-231, MIA PaCa-2, and HCT-15) were labeled with 10 μg/mL of Calcein AM (Thermo). The target cells were plated in 96-well plates at a density of 5 × 10^3 cells/well and combined with effector cells (effector-to-target ratio, 50:1) and 100 μg/mL of either control mIgG$_{2a}$ or Ea$_2$Mab-7-mG$_{2a}$, either control hIgG$_1$ or Ea$_2$Mab-7-hG$_1$. After incubating for 4.5 hours at 37°C, the calcein released into the supernatant was measured as described previously [36]..

2.6. CDC

The target cells labeled with Calcein AM (MDA-MB-231, MIA PaCa-2, and HCT-15) were seeded and combined with rabbit complement (final concentration 10%, Low-Tox-M Rabbit Complement; Cedarlane Laboratories, Hornby, ON, Canada) along with 100 μg/mL of either control mIgG$_{2a}$ or Ea$_2$Mab-7-mG$_{2a}$, either control hIgG$_1$ or Ea$_2$Mab-7-hG$_1$. After a 4.5-hour incubation at 37°C, the amount of calcein released into the medium was measured as described previously [36].

2.7. Antitumor Activities in Xenografts of Human Tumors

MDA-MB-231, MIA PaCa-2, and HCT-15 were mixed with Matrigel Matrix Growth Factor Reduced (BD Biosciences). Subcutaneous injections (5 × 10^6 cells/mouse) were then given to the left flanks of BALB/c nude mice. On the seventh post-inoculation day, 100 μg of control mIgG$_{2a}$ (n = 8), Ea$_2$Mab-7-mG$_{2a}$ (n = 8), control hIgG$_1$ (n = 8), or Ea$_2$Mab-7-hG$_1$ (n = 8) in 100 μL PBS were administered intraperitoneally. Additional antibody injections were given on day 14. The tumor diameter was assessed on days 7, 14, 16, and 21 after the tumor cell implantation. Tumor volume was calculated using the formula: volume = W^2 × L/2, where W represents the short diameter and L the long diameter. The mice's weight was also assessed on days 7, 14, 16, and 21 following tumor cell inoculation. When observations on day 21 were complete, the mice were sacrificed, and tumor weights were assessed after tumor excision.

2.8. Statistical Analyses

The mean ± standard error of the mean (SEM) is presented in all data. A two-tailed unpaired t-test was conducted to measure ADCC, CDC, and tumor weight. ANOVA with Sidak's post hoc test

 doi:10.20944/preprints202512.0860.v1

was performed for tumor volume and mouse weight. GraphPad Prism 10 (GraphPad Software, Inc., La Jolla, CA, USA) was used for all calculations. $p < 0.05$ was considered statistically significant.

3. Results

3.1. Production of Class-Switched mAbs from Ea2Mab-7

We previously reported that Ea2Mab-7, an anti-EphA2 mAb, detects EphA2-positive cells by flow cytometry, western blotting, and immunohistochemistry[37]. We first confirmed the specificity of Ea2Mab-7 using nine EphA and five EphB receptors-overexpressed CHO-K1 [31]. As shown in supplementary Fig. 1, Ea2Mab-7 showed the binding to CHO/EphA2, with no or very little cross-reactivity to other Eph receptors observed at 10 μg/mL. We next determined the V_H and V_L CDR sequences of Ea2Mab-7 (Fig. 1A). Furthermore, we engineered a mouse IgG2a-type Ea2Mab-7 (Ea2Mab-7-mG2a) and human IgG1-type Ea2Mab-7 (Ea2Mab-7-hG1) by fusing the V_H and V_L CDRs of Ea2Mab-7 with the C_H and C_L chains of mouse IgG2a and human IgG1, respectively (Fig. 1A). Isotype control mAbs, PMab-231 (mouse IgG2a, referred to as control mIgG2a) and humCvMab-62 (human IgG1, referred to as control hIgG1) were also prepared. Under reduced conditions, we confirmed the purity of original and recombinant mAbs by SDS-PAGE (Fig. 1B).

Next, the binding affinity was investigated using flow cytometry. The dissociation constant (K_D) values of Ea2Mab-7-mG2a and Ea2Mab-7-hG1 for CHO/EphA2 were determined to be 4.6×10^{-9} M and 3.3×10^{-9} M, respectively (Fig. 1C). These results indicated that Ea2Mab-7-mG2a and Ea2Mab-7-hG1 retain the affinity with parental mAb, Ea2Mab-7 as reported previously (K_D: 6.2×10^{-9} M) [30].

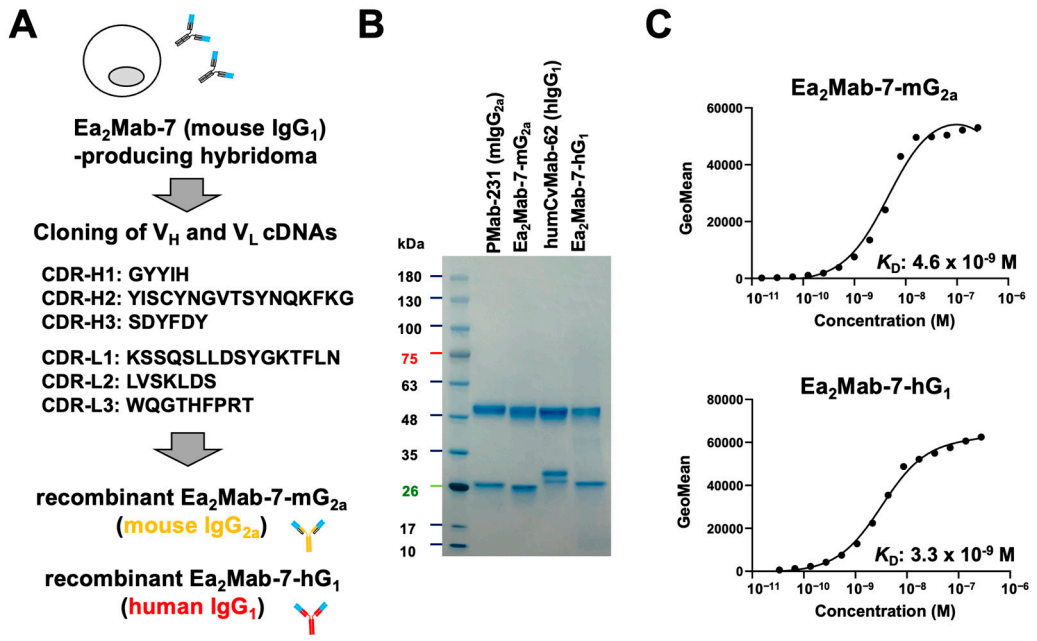

Figure 1. Production of Ea2Mab-7-mG2a and Ea2Mab-7-hG1. (**A**) After determination of CDRs of Ea2Mab-7 (mouse IgG1), recombinant Ea2Mab-7-mG2a (mouse IgG2a) and Ea2Mab-7-hG1 (human IgG1) were produced. The amino acid sequence of V_H and V_L CDRs was indicated. (**B**) PMab-231 (control mIgG2a), Ea2Mab-7-mG2a, humCvMab-62 (control hIgG1), and Ea2Mab-7-hG1 were subject to SDS-PAGE, and the gel was stained with Bio-Safe CBB G-250 Stain. (**C**) Determination of the binding affinity of Ea2Mab-7-mG2a and Ea2Mab-7-hG1 using flow cytometry. CHO/EphA2 was suspended in Ea2Mab-7-mG2a and Ea2Mab-7-hG1 at indicated concentrations, followed by Alexa Fluor 488-conjugated anti-mouse IgG treatment. The SA3800 Cell Analyzer was used to analyze fluorescence data. The dissociation constant (K_D) values were determined using GraphPad Prism 6.

3.2. Flow Cytometry Using Ea2Mab-7-mG2a and Ea2Mab-7-hG1 in EphA2-Positive Cancer Cells

We next screened the EphA2 expression in more than 100 cell lines using flow cytometry. Among them, we chose human TNBC MDA-MB-231, pancreas cancer MIA PaCa-2, and colorectal cancer HCT-15 based on their reactivity and availability in mouse xenograft models. As shown in Fig. 2A-

 doi:10.20944/preprints202512.0860.v1

C, Ea2Mab-7-mG2a recognized with MDA-MB-231, MIA PaCa-2, and HCT-15 in flow cytometry at 0.1 μg/mL. In contrast, control mIgG2a did not. Ea2Mab-7-hG1 also showed similar reactivity at 0.1 μg/mL, but control hIgG1 did not (Fig. 2A-C). The dissociation constant (K_D) values of Ea2Mab-7-mG2a and Ea2Mab-7-hG1 for MDA-MB-231 were determined to be 7.4×10^{-10} M and 5.5×10^{-9} M, respectively (Fig. 2D). These results indicated that both Ea2Mab-7-mG2a and Ea2Mab-7-hG1 exhibit high binding affinity for MDA-MB-231.

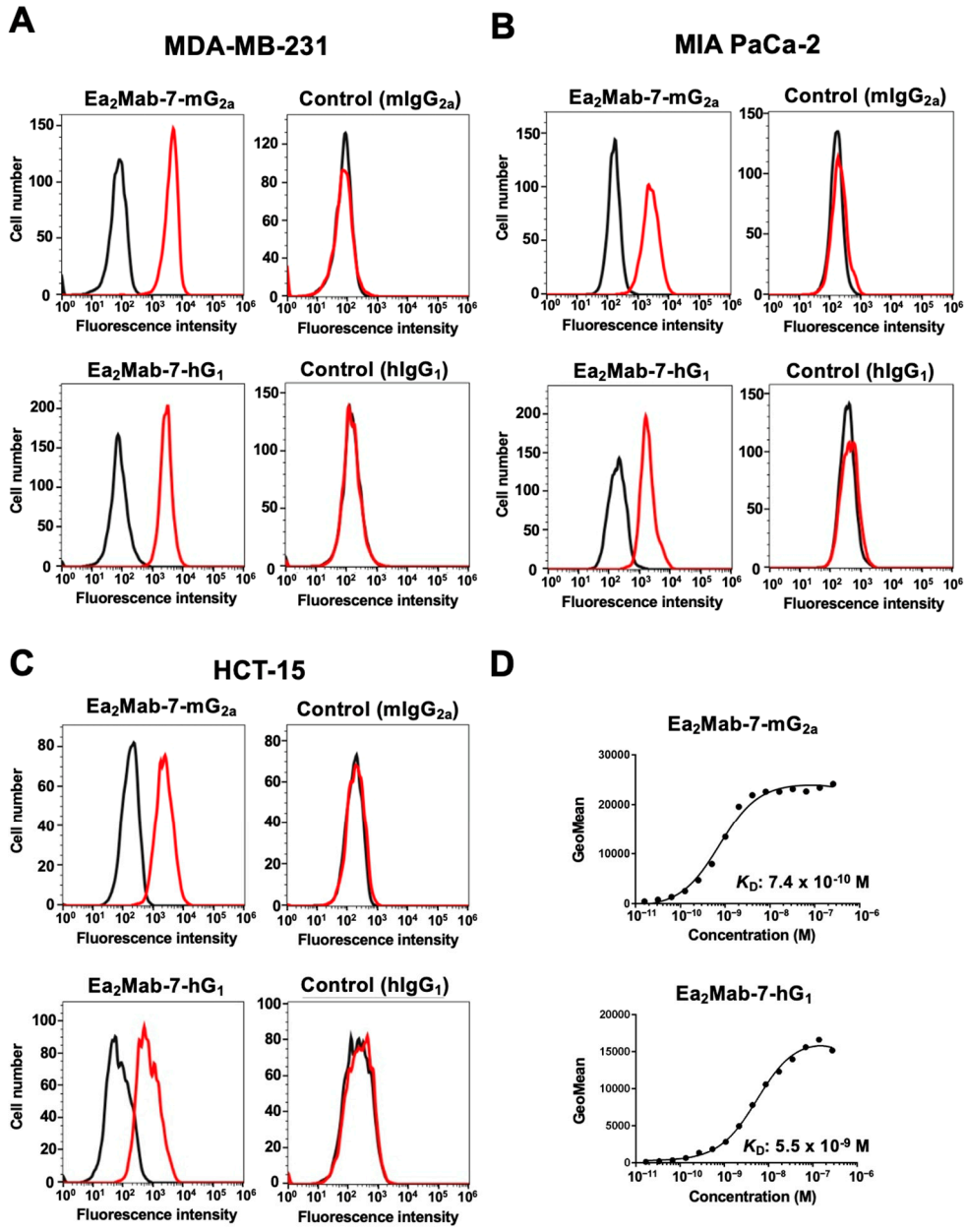

Figure 2. Reactivity of Ea2Mab-7-mG2a and Ea2Mab-7-hG1 to tumor cells. (**A-C**) Flow cytometry using control mIgG2a, Ea2Mab-7-mG2a, control hIgG1, and Ea2Mab-7-hG1 (0.1 μg/mL; Red line) or buffer control (Black line) against breast cancer MDA-MB-231 (**A**), pancreatic cancer MIA PaCa-2 (**B**), and colorectal cancer HCT-15 (**C**). After treatment with primary mAbs, cells were treated with Alexa Fluor 488-conjugated anti-mouse IgG. (**D**) Determination of the binding affinity of Ea2Mab-7-mG2a and Ea2Mab-7-hG1 using flow cytometry. MDA-MB-231 was suspended in Ea2Mab-7-mG2a and Ea2Mab-7-hG1 at indicated concentrations, followed by Alexa Fluor 488-conjugated anti-mouse IgG treatment. Fluorescence data were analyzed using the SA3800 Cell Analyzer. The dissociation constant (K_D) values were determined using GraphPad Prism 6.

3.3. ADCC and CDC Elicited by Ea2Mab-7-mG2a Against EphA2-Positive Cancer Cells

 doi:10.20944/preprints202512.0860.v1

We next investigated whether Ea2Mab-7-mG2a exhibits ADCC and CDC against EphA2-positive MDA-MB-231, MIA PaCa-2, and HCT-15 cells. The ADCC induced by Ea2Mab-7-mG2a and control mIgG2a was investigated in the presence of effector splenocytes derived from BALB/c nude mice. As shown in Figure 3A, Ea2Mab-7-mG2a induced potent ADCC against MDA-MB-231 (34.4% cytotoxicity; $p < 0.05$) compared to the control mIgG2a (8.7% cytotoxicity). Ea2Mab-7-mG2a elicited ADCC against MIA PaCa-2 (9.0% cytotoxicity; $p < 0.05$) more effectively than the control mIgG2a (2.3% cytotoxicity). Furthermore, Ea2Mab-7-mG2a also showed potent ADCC against HCT-15 (38.7% cytotoxicity; $p < 0.05$) more effectively than the control mIgG2a (9.2% cytotoxicity).

The CDC elicited by Ea2Mab-7-mG2a was next investigated in the presence of complements. As shown in Figure 3B, Ea2Mab-7-mG2a elicited significant CDC against MDA-MB-231 (14.8% cytotoxicity; $p < 0.05$) compared to the control mIgG2a (2.8% cytotoxicity). Ea2Mab-7-mG2a induced potent CDC against MIA PaCa-2 (25.8% cytotoxicity; $p < 0.01$) more effectively than the control mIgG2a (1.0% cytotoxicity). Additionally, Ea2Mab-7-mG2a showed CDC against HCT-15 (14.8% cytotoxicity; $p < 0.01$) more effectively than the control mIgG2a (2.8% cytotoxicity).

These results indicated that Ea2Mab-7-mG2a exerted ADCC and CDC in the presence of effector splenocytes and complements, respectively.

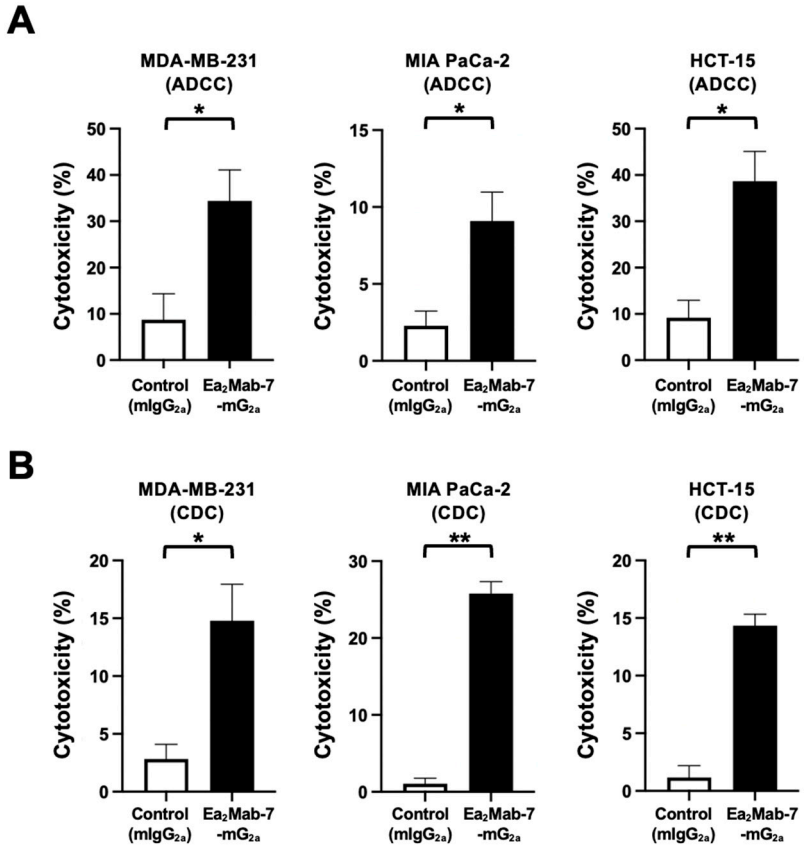

Figure 3. ADCC and CDC by Ea2Mab-7-mG2a against EphA2-positive tumor cells. The target cells labeled with Calcein AM (MDA-MB-231, MIA PaCa-2, and HCT-15) were incubated with effector splenocyte derived from BALB/c nude mice (**A**) or rabbit complement (**B**) in the presence of Ea2Mab-7-mG2a or control mIgG2a. Calcein release into the medium was measured, and cytotoxicity was determined. Values are shown as the mean ± SEM. Asterisks indicate statistical significance (* $p < 0.05$; two-tailed unpaired t-test).

3.4. Antitumor effects of Ea2Mab-7-mG2a Against EphA2-Positive Cancer Cells

After the inoculation of MDA-MB-231, MIA PaCa-2, or HCT-15 at the left flanks of BALB/c nude mice, Ea2Mab-7-mG2a or control mIgG2a was intraperitoneally injected into the xenograft-bearing mice on days 7 and 14. The tumor volume was measured on the indicated days. The Ea2Mab-7-mG2a administration resulted in a significant reduction in MDA-MB-231 xenografts on days 14 ($p < 0.05$) and 21 ($p < 0.01$) compared with that of control mIgG2a (Figure 4A). In the MIA PaCa-2 xenograft, a

 doi:10.20944/preprints202512.0860.v1

significant reduction was observed on day 21 ($p < 0.01$) (Figure 4B). In the HCT-15 xenograft, a significant reduction was also observed on days 14 ($p < 0.05$), 16 ($p < 0.05$), and 21 ($p < 0.05$) (Figure 4C).

In the xenograft weight, Ea2Mab-7-mG2a showed the reduction in MDA-MB-231 (60% reduction; $p < 0.01$; Figure 4D), MIA PaCa-2 (22% reduction; $p < 0.05$; Figure 4E), and HCT-15 (17% reduction; $p < 0.01$; Figure 4F) compared with control mIgG2a. The resected MDA-MB-231, MIA PaCa-2, and HCT-15 tumors on day 21 are shown in each figure. The xenograft-bearing mice did not lose body weight by Ea2Mab-7-mG2a treatment (Figure 4G–I).

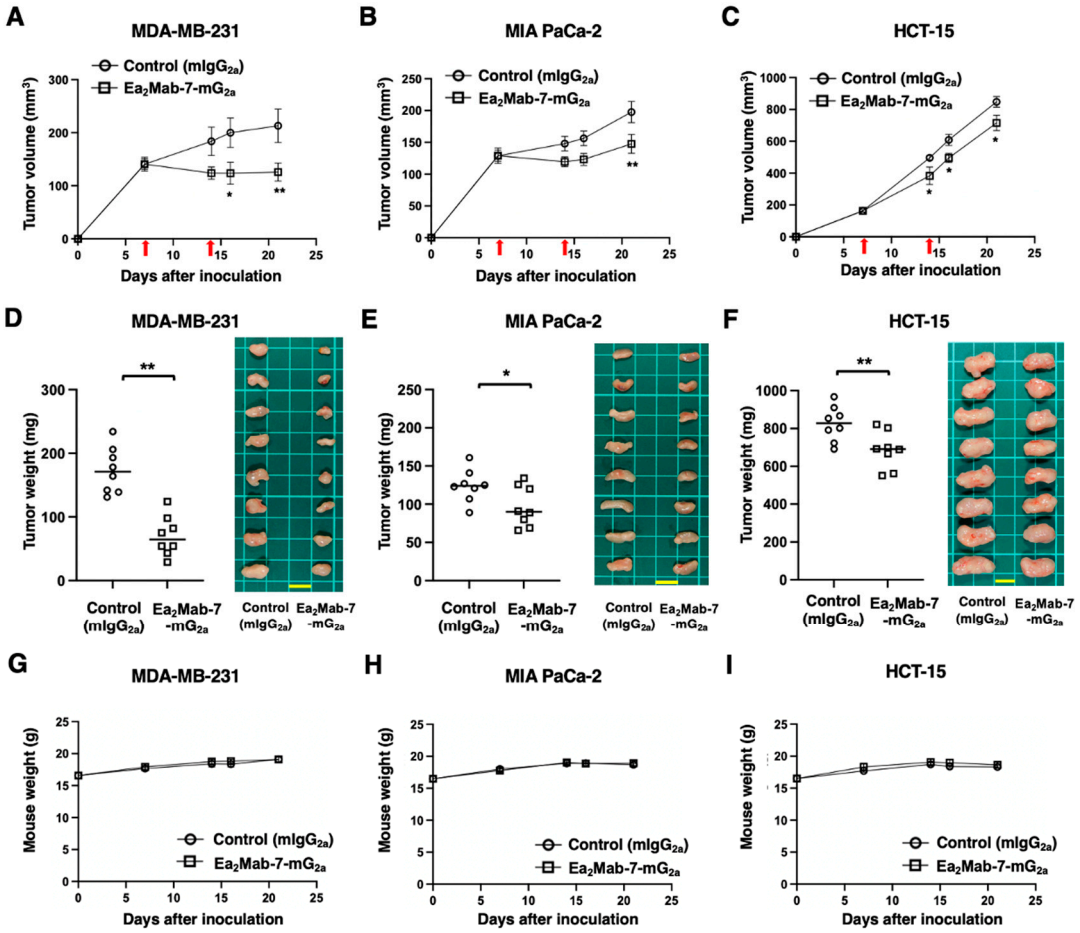

Figure 4. Antitumor activity of Ea2Mab-7-mG2a against human tumor xenografts. (**A–C**) MDA-MB-231 (**A**), MIA PaCa-2 (**B**), and HCT-15 (**C**) cells were subcutaneously injected into BALB/c nude mice (day 0). Ea2Mab-7-mG2a (100 μg) or control mIgG2a (100 μg) were intraperitoneally injected into each mouse on days 7 and 14 (arrows). The tumor volume is represented as the mean ± SEM. * $p < 0.05$, ** $p < 0.01$ (two-way ANOVA with Sidak's post hoc test). (**D–F**) After cell inoculation, the mice were euthanized on day 21. The tumor weights (left) and appearance (right) of MDA-MB-231 (**D**), MIA PaCa-2 (**E**), and HCT-15 (**F**) xenografts were measured. Values are presented as the mean ± SEM. ** $p < 0.01$ and * $p < 0.05$ (two-tailed unpaired t-test). Scale bar, 1 cm. (**G-I**) Body weight (mean ± SEM) of xenograft-bearing mice treated with the mAbs is presented. There is no significant difference (two-way ANOVA with Sidak's post hoc test).

3.5. ADCC and CDC Elicited by Ea2Mab-7-hG1 Against EphA2-Positive Cancer Cells

We next investigated whether Ea2Mab-7-hG1 exhibits ADCC and CDC against EphA2-positive MDA-MB-231, MIA PaCa-2, and HCT-15. We also used the BALB/c nude mice-derived splenocytes as effector cells because all four mouse Fcγ receptors bind to human IgG1, which induces ADCC in the presence of mouse effector cells [38]. Therefore, the ADCC induced by Ea2Mab-7-hG1 and control hIgG1 was investigated in the presence of BALB/c nude mice-derived splenocytes. As shown in Figure 5A, Ea2Mab-7-hG1 induced potent ADCC against MDA-MB-231 (35.3% cytotoxicity; $p < 0.05$) compared to the control hIgG1 (14.0% cytotoxicity). Ea2Mab-7-hG1 elicited ADCC against MIA PaCa-

 doi:10.20944/preprints202512.0860.v1

2 (8.4% cytotoxicity; $p < 0.01$) more effectively than the control hIgG$_1$ (1.6% cytotoxicity). Furthermore, Ea$_2$Mab-7-hG$_1$ also showed potent ADCC against HCT-15 (32.6% cytotoxicity; $p < 0.01$) more effectively than the control hIgG$_1$ (7.3% cytotoxicity).

The CDC elicited by Ea$_2$Mab-7-hG$_1$ was next investigated in the presence of complements. As shown in Figure 5B, Ea$_2$Mab-7-hG$_1$ elicited significant CDC against MDA-MB-231 (13.4% cytotoxicity; $p < 0.01$) compared to the control hIgG$_1$ (3.5% cytotoxicity). Ea$_2$Mab-7-hG$_1$ induced potent CDC against MIA PaCa-2 (18.8% cytotoxicity; $p < 0.01$) more effectively than the control hIgG$_1$ (1.3% cytotoxicity). Additionally, Ea$_2$Mab-7-hG$_1$ showed CDC against HCT-15 (7.1% cytotoxicity; $p < 0.05$) more effectively than the control hIgG$_1$ (2.8% cytotoxicity).

These results indicated that Ea$_2$Mab-7-hG$_1$ exerted ADCC and CDC in the presence of effector splenocytes and complements, respectively.

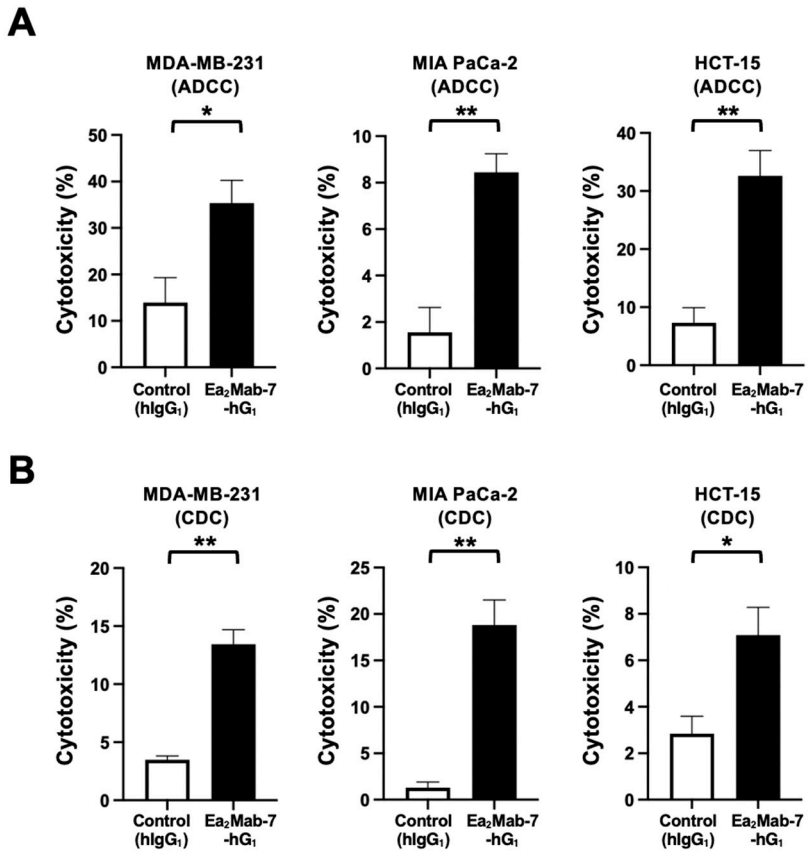

Figure 5. ADCC and CDC by Ea$_2$Mab-7-hG$_1$ against EphA2-positive tumor cells. The target cells labeled with Calcein AM (MDA-MB-231, MIA PaCa-2, and HCT-15) were incubated with effector splenocyte derived from BALB/c nude mice (**A**) or rabbit complement (**B**) in the presence of Ea$_2$Mab-7-hG$_1$ or control hIgG$_1$. Calcein release into the medium was measured, and cytotoxicity was determined. Values are shown as the mean ± SEM. Asterisks indicate statistical significance (* $p < 0.05$; two-tailed unpaired *t*-test).

3.6. Antitumor Effects of Ea$_2$Mab-7-hG$_1$ Against EphA2-Positive Cancer Cells

In preclinical studies of clinically approved mAbs, such as trastuzumab (human IgG$_1$), the antitumor efficacy was demonstrated in nude mice bearing breast cancer xenografts in the absence of human-derived effectors [39-41]. Therefore, the antitumor effect of Ea$_2$Mab-7-hG$_1$ was examined in cancer xenografts inoculated in nude mice. After the inoculation of MDA-MB-231, MIA PaCa-2, or HCT-15 at the left flanks of BALB/c nude mice, Ea$_2$Mab-7-hG$_1$ or control hIgG$_1$ was intraperitoneally injected into the xenograft-bearing mice on days 7 and 14. The tumor volume was measured on the indicated days. The Ea$_2$Mab-7-hG$_1$ administration resulted in a potent reduction in MDA-MB-231 xenografts on days 14 ($p < 0.01$), 16 ($p < 0.01$), and 21 ($p < 0.01$) compared with that of control hIgG$_1$ (Figure 6A). In the MIA PaCa-2 xenograft, a significant reduction was observed on day 21 ($p < 0.05$)

 doi:10.20944/preprints202512.0860.v1

(Figure 6B). In the HCT-15 xenograft, a significant reduction was also observed on days 16 ($p < 0.05$) and 21 ($p < 0.01$) (Figure 6C).

In the xenograft weight, Ea2Mab-7-hG1 showed the reduction in MDA-MB-231 (56% reduction; $p < 0.01$; Figure 6D), MIA PaCa-2 (38% reduction; $p < 0.01$; Figure 6E), and HCT-15 (26% reduction; $p < 0.01$; Figure 6F) compared with control hIgG1. The resected MDA-MB-231, MIA PaCa-2, and HCT-15 tumors on day 21 are shown in each figure. The xenograft-bearing mice did not lose body weight by Ea2Mab-7-hG1 treatment (Figure 6G–I).

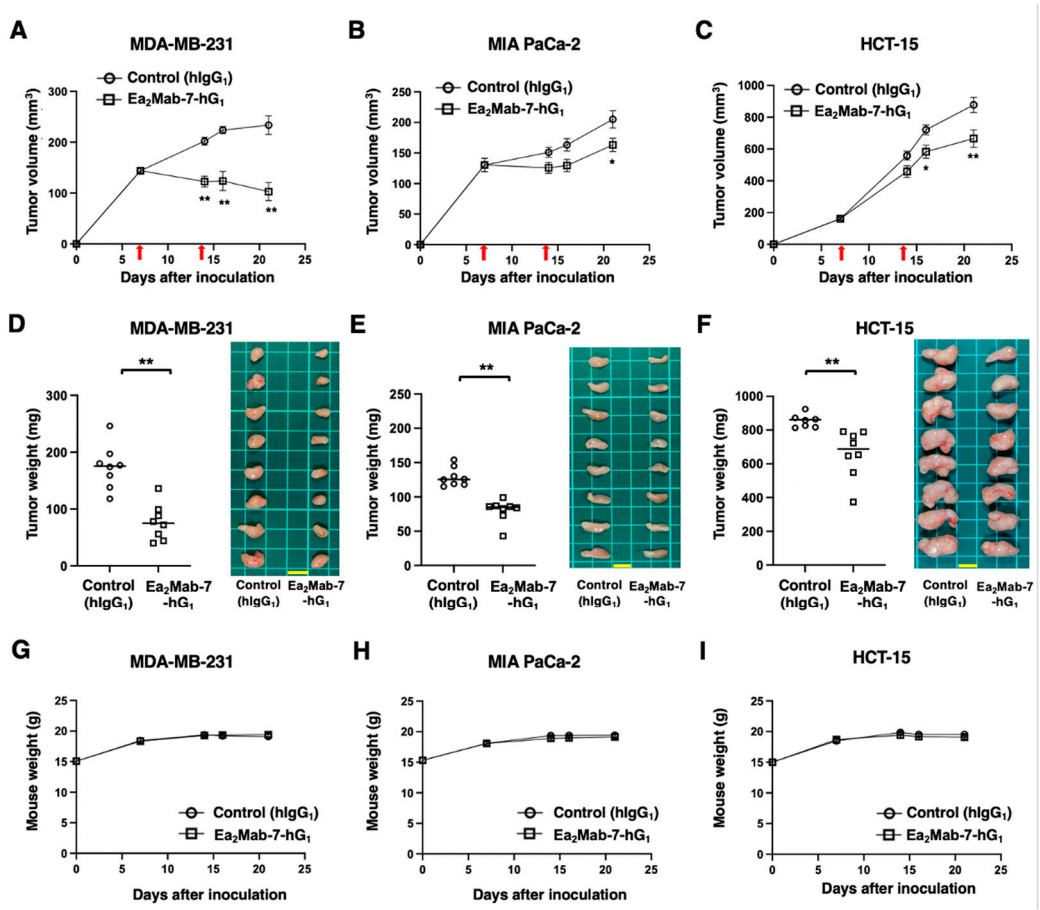

Figure 6. Antitumor activity of Ea2Mab-7-hG1 against human tumor xenografts. (**A**–**C**) MDA-MB-231 (**A**), MIA PaCa-2 (**B**), and HCT-15 (**C**) cells were subcutaneously injected into BALB/c nude mice (day 0). Ea2Mab-7-hG1 (100 μg) or control hIgG1 (100 μg) were intraperitoneally injected into each mouse on days 7 and 14 (arrows). The tumor volume is represented as the mean ± SEM. * $p < 0.05$, ** $p < 0.01$ (two-way ANOVA with Sidak's post hoc test). (**D**–**F**) After cell inoculation, the mice were euthanized on day 21. The tumor weights (left) and appearance (right) of MDA-MB-231 (**D**), MIA PaCa-2 (**E**), and HCT-15 (**F**) xenografts were measured. Values are presented as the mean ± SEM. ** $p < 0.01$ (two-tailed unpaired *t*-test). Scale bar, 1 cm. (**G-I**) Body weight (mean ± SEM) of xenograft-bearing mice treated with the mAbs is presented. There is no significant difference (two-way ANOVA with Sidak's post hoc test).

4. Discussion

This study demonstrated the *in vitro* and *in vivo* antitumor efficacy of a novel mAb against EphA2. Both Ea2Mab-7-mG2a and Ea2Mab-7-hG1 recognized MDA-MB-231, MIA PaCa-2, and HCT-15 in flow cytometry (Fig. 2). We compared the ADCC, CDC (Fig. 3 and 5), and *in vivo* antitumor effect (Fig. 4 and 6) between Ea2Mab-7-mG2a and Ea2Mab-7-hG1 in the same experimental setting. Although the binding affinity to MDA-MB-231 differed between Ea2Mab-7-mG2a and Ea2Mab-7-hG1 (Fig. 2D), the *in vitro* and *in vivo* efficacy was similar, suggesting that Ea2Mab-7-hG1 activated the effectors and exhibited antitumor efficacy in mice.

DS-8895a, an afucosylated anti-EphA2 mAb, was previously developed to potentiate ADCC [26]. However, the clinical trial of DS-8895a was terminated due to low tumor uptake and therapeutic

 doi:10.20944/preprints202512.0860.v1

efficacy in advanced solid tumor patients [29,42]. Therefore, selecting tumor samples and/or measuring EphA2 abundance are thought to be essential. Since Ea$_2$Mab-7 is suitable for detecting EphA2 in immunohistochemistry using a clinically approved staining system [30], the validation of EphA2 expression by Ea$_2$Mab-7 is necessary in future studies.

In metastatic colorectal cancer, EphA2 levels are significantly associated with worse outcome in patients treated with FOLFIRI plus cetuximab, an anti-EGFR mAb [43]. In HCT-15 xenograft models, ALW-II-41-27 (an EphA2 tyrosine kinase inhibitor) and cetuximab synergistically inhibited the xenograft growth [43]. Therefore, the combined effect of Ea$_2$Mab-7-mG$_{2a}$ or Ea$_2$Mab-7-hG$_1$ with cetuximab should be evaluated in preclinical models.

In pancreatic ductal adenocarcinoma (PDAC), EphA2 was identified as a candidate tumor-intrinsic driver of immunosuppression [44]. EphA2 expression in PDAC promotes an immunosuppressive tumor microenvironment that confers resistance to combination immunotherapy [44]. Since the EphA2-prostaglandin endoperoxide synthase 2 (PTGS2) axis mediated the T cell exclusion and was associated with poor patient survival, the blockade by anti-EphA2 mAbs may represent a therapeutic strategy for immunotherapy-resistant PDAC. Ea$_2$Mab-7-mG$_{2a}$ or Ea$_2$Mab-7-hG$_1$ should be evaluated to determine whether they possess the inhibitory effect of the EphA2-PTGS2 axis and evaluate the antitumor effect in combination with immunotherapy.

The oncogenic herpesviruses such as Epstein-Barr virus (EBV) persistently infect over 90% of adults worldwide, leading to the development of B cell or epithelial malignancies [45]. EBV is responsible for approximately 2% of all cancers, including lymphomas (e.g., Burkitt's lymphoma and Hodgkin's lymphoma) and carcinomas (e.g., nasopharyngeal, gastric, and breast cancers) [46,47]. Studies have reported that EBV-associated carcinomas arise from clonal expansion of infected cells, suggesting that early infection events are sufficient to initiate carcinogenesis [48]. EBV utilizes different viral glycoproteins and distinct host receptors to infect human B cells and epithelial cells [49]. EBV entry into an epithelial cell involves different attachment and fusion proteins mediated by interactions between viral glycoproteins (gH/gL, gB) and host receptors, EphA2 [50] and R9AP (RGS9-1 anchor protein) [51]. In epithelial cells, gH/gL simultaneously binds to EphA2 and R9AP, which leads to gB-mediated viral and host membrane fusion [51]. Ganoderma microsporum immunomodulatory protein interacts with the gB and the host epithelial receptor EphA2, which disrupt viral and host membrane fusion [52]. Although the neutralizing effect of anti-EphA2 mAbs on EBV infection has not been evaluated, anti-EphA2 mAbs, including Ea$_2$Mab-7-mG$_{2a}$ and Ea$_2$Mab-7-hG$_1$, have the potential to control the infection and tumorigenesis in EBV-associated carcinomas.

A clinical trial of MEDI-547, an anti-EphA2 mAb-ADC, was discontinued due to the unacceptable toxicities [27]. Since EphA2 is expressed in various types of normal cells, these anti-EphA2 mAbs may recognize normal cells. As shown in supplementary Fig. 2, Ea$_2$Mab-7 recognized normal fibroblast (KMST-6) and epithelial cell lines (293FT and hTCEpi) in flow cytometry. Therefore, cancer-specific mAbs (CasMabs) for EphA2 should be selected to achieve an acceptable therapeutic window with low on-target toxicity.

Our group has developed CasMabs for various antigens, including podoplanin, podocalyxin, and human epidermal growth factor receptor 2 (HER2), and has clarified the cancer-specific epitopes. In the anti-HER2 CasMab development, we selected an anti-HER2 CasMab, H$_2$CasMab-2 (also known as H2Mab-250) from about three hundred anti-HER2 mAb clones [32]. H$_2$CasMab-2 recognized HER2 in breast cancer cells but not in regular epithelial cell lines derived from the mammary gland, colon, kidney proximal tubule, and lung bronchus[32]. The epitope analyses identified a critical amino acid (Trp614) in the HER2 extracellular domain for H$_2$CasMab-2 recognition [32] and solved the structure of cancer-specific recognition [53]. Furthermore, a single-chain variable fragment of H$_2$CasMab-2 was developed to chimeric antigen receptor (CAR)-T cell therapy, which exhibited cancer-specific reactivity and antitumor efficacy [53]. The H$_2$CasMab-2 CAR-T is currently being evaluated in a phase I clinical trial for patients with HER2-positive advanced solid tumors (NCT06241456) [53]. Therefore, selecting CasMab against EphA2 and identifying the cancer-specific epitopes are essential strategies for developing therapeutic mAbs and modalities. We have developed about 100 clones of Ea$_2$Mabs and will screen for cancer-specific reactivity. Ea$_2$Mab-7-mG$_{2a}$ and Ea$_2$Mab-7-hG$_1$ would serve as reference mAbs to compare the antitumor efficacy with anti-EphA2 CasMabs.

 doi:10.20944/preprints202512.0860.v1

Supplementary Materials: The following supporting information can be downloaded at the website of this paper posted on Preprints.org.

Author Contributions: Conceptualization, M.K.K. and Y.K.; methodology, M.K.K. and T.O.; validation, H.S. and Y.K.; investigation, A.H., G.L., T.O., H.S., K.I., K.S., A.N., H.A., N.K., K.S., S.H., T.N., M.Y., T.T., and H.S.; data curation, H.S.; writing—original draft preparation, G.L. and H.S.; writing—review and editing, Y.K.; project administration, Y.K.; funding acquisition, Y.K. All authors have read and agreed to the published version of the manuscript.

Funding: This research was supported in part by Japan Agency for Medical Research and Development (AMED) under Grant Numbers: JP25am0521010 (to Y.K.), JP25ama121008 (to Y.K.), JP25ama221153 (to Y.K.), JP25ama221339 (to Y.K.), and JP25bm1123027 (to Y.K.), and by the Japan Society for the Promotion of Science (JSPS) Grants-in-Aid for Scientific Research (KAKENHI) grant nos. 25K18843 (to G.L.), 24K11652 (to H. Satofuka), 24K18268 (to T.T.), and 25K10553 (to Y.K.).

Institutional Review Board Statement: The Institutional Committee for Experiments of the Institute of Microbial Chemistry approved animal experiments (approval no. 2025-040).

Informed Consent Statement: Not applicable.

Data Availability Statement: The data presented in this study are available in the article.

Conflicts of Interest: The authors declare no conflict of interest.

References

1. Pasquale, E.B. Eph receptors and ephrins in cancer progression. *Nat Rev Cancer* **2024**, *24*, 5-27, doi:10.1038/s41568-023-00634-x.
2. Miao, H.; Wang, B. EphA receptor signaling--complexity and emerging themes. *Semin Cell Dev Biol* **2012**, *23*, 16-25, doi:10.1016/j.semcdb.2011.10.013.
3. Pasquale, E.B. Eph-ephrin bidirectional signaling in physiology and disease. *Cell* **2008**, *133*, 38-52, doi:10.1016/j.cell.2008.03.011.
4. Pasquale, E.B. Eph receptor signalling casts a wide net on cell behaviour. *Nat Rev Mol Cell Biol* **2005**, *6*, 462-475, doi:10.1038/nrm1662.
5. Zhu, Y.; Su, S.A.; Shen, J.; Ma, H.; Le, J.; Xie, Y.; Xiang, M. Recent advances of the Ephrin and Eph family in cardiovascular development and pathologies. *iScience* **2024**, *27*, 110556, doi:10.1016/j.isci.2024.110556.
6. Lévy, J.; Schell, B.; Nasser, H.; Rachid, M.; Ruaud, L.; Couque, N.; Callier, P.; Faivre, L.; Marle, N.; Engwerda, A.; et al. EPHA7 haploinsufficiency is associated with a neurodevelopmental disorder. *Clin Genet* **2021**, *100*, 396-404, doi:10.1111/cge.14017.
7. Yang, Y.; Ding, T.; Cong, Y.; Luo, X.; Liu, C.; Gong, T.; Zhao, M.; Zheng, X.; Li, C.; Zhang, Y.; et al. Interferon-induced transmembrane protein-1 competitively blocks Ephrin receptor A2-mediated Epstein-Barr virus entry into epithelial cells. *Nat Microbiol* **2024**, *9*, 1256-1270, doi:10.1038/s41564-024-01659-0.
8. Miao, H.; Li, D.Q.; Mukherjee, A.; Guo, H.; Petty, A.; Cutter, J.; Basilion, J.P.; Sedor, J.; Wu, J.; Danielpour, D.; et al. EphA2 mediates ligand-dependent inhibition and ligand-independent promotion of cell migration and invasion via a reciprocal regulatory loop with Akt. *Cancer Cell* **2009**, *16*, 9-20, doi:10.1016/j.ccr.2009.04.009.
9. Toracchio, L.; Carrabotta, M.; Mancarella, C.; Morrione, A.; Scotlandi, K. EphA2 in Cancer: Molecular Complexity and Therapeutic Opportunities. *Int J Mol Sci* **2024**, *25*, doi:10.3390/ijms252212191.
10. Boyd, A.W.; Bartlett, P.F.; Lackmann, M. Therapeutic targeting of EPH receptors and their ligands. *Nat Rev Drug Discov* **2014**, *13*, 39-62, doi:10.1038/nrd4175.
11. Pasquale, E.B. Eph receptors and ephrins in cancer: bidirectional signalling and beyond. *Nat Rev Cancer* **2010**, *10*, 165-180, doi:10.1038/nrc2806.
12. Lechtenberg, B.C.; Gehring, M.P.; Light, T.P.; Horne, C.R.; Matsumoto, M.W.; Hristova, K.; Pasquale, E.B. Regulation of the EphA2 receptor intracellular region by phosphomimetic negative charges in the kinase-SAM linker. *Nat Commun* **2021**, *12*, 7047, doi:10.1038/s41467-021-27343-z.

 doi:10.20944/preprints202512.0860.v1

13. Zhou, Y.; Yamada, N.; Tanaka, T.; Hori, T.; Yokoyama, S.; Hayakawa, Y.; Yano, S.; Fukuoka, J.; Koizumi, K.; Saiki, I.; et al. Crucial roles of RSK in cell motility by catalysing serine phosphorylation of EphA2. *Nat Commun* **2015**, *6*, 7679, doi:10.1038/ncomms8679.
14. Barquilla, A.; Lamberto, I.; Noberini, R.; Heynen-Genel, S.; Brill, L.M.; Pasquale, E.B. Protein kinase A can block EphA2 receptor-mediated cell repulsion by increasing EphA2 S897 phosphorylation. *Mol Biol Cell* **2016**, *27*, 2757-2770, doi:10.1091/mbc.E16-01-0048.
15. Porazinski, S.; de Navascués, J.; Yako, Y.; Hill, W.; Jones, M.R.; Maddison, R.; Fujita, Y.; Hogan, C. EphA2 Drives the Segregation of Ras-Transformed Epithelial Cells from Normal Neighbors. *Curr Biol* **2016**, *26*, 3220-3229, doi:10.1016/j.cub.2016.09.037.
16. Harly, C.; Joyce, S.P.; Domblides, C.; Bachelet, T.; Pitard, V.; Mannat, C.; Pappalardo, A.; Couzi, L.; Netzer, S.; Massara, L.; et al. Human γδ T cell sensing of AMPK-dependent metabolic tumor reprogramming through TCR recognition of EphA2. *Sci Immunol* **2021**, *6*, doi:10.1126/sciimmunol.aba9010.
17. Cioce, M.; Fazio, V.M. EphA2 and EGFR: Friends in Life, Partners in Crime. Can EphA2 Be a Predictive Biomarker of Response to Anti-EGFR Agents? *Cancers (Basel)* **2021**, *13*, doi:10.3390/cancers13040700.
18. Amato, K.R.; Wang, S.; Tan, L.; Hastings, A.K.; Song, W.; Lovly, C.M.; Meador, C.B.; Ye, F.; Lu, P.; Balko, J.M.; et al. EPHA2 Blockade Overcomes Acquired Resistance to EGFR Kinase Inhibitors in Lung Cancer. *Cancer Res* **2016**, *76*, 305-318, doi:10.1158/0008-5472.Can-15-0717.
19. Paraiso, K.H.; Das Thakur, M.; Fang, B.; Koomen, J.M.; Fedorenko, I.V.; John, J.K.; Tsao, H.; Flaherty, K.T.; Sondak, V.K.; Messina, J.L.; et al. Ligand-independent EPHA2 signaling drives the adoption of a targeted therapy-mediated metastatic melanoma phenotype. *Cancer Discov* **2015**, *5*, 264-273, doi:10.1158/2159-8290.Cd-14-0293.
20. Volz, C.; Breid, S.; Selenz, C.; Zaplatina, A.; Golfmann, K.; Meder, L.; Dietlein, F.; Borchmann, S.; Chatterjee, S.; Siobal, M.; et al. Inhibition of Tumor VEGFR2 Induces Serine 897 EphA2-Dependent Tumor Cell Invasion and Metastasis in NSCLC. *Cell Rep* **2020**, *31*, 107568, doi:10.1016/j.celrep.2020.107568.
21. Mitra, D.; Bhattacharyya, S.; Alam, N.; Sen, S.; Mitra, S.; Mandal, S.; Vignesh, S.; Majumder, B.; Murmu, N. Phosphorylation of EphA2 receptor and vasculogenic mimicry is an indicator of poor prognosis in invasive carcinoma of the breast. *Breast Cancer Res Treat* **2020**, *179*, 359-370, doi:10.1007/s10549-019-05482-8.
22. Van den Broeck, A.; Vankelecom, H.; Van Eijsden, R.; Govaere, O.; Topal, B. Molecular markers associated with outcome and metastasis in human pancreatic cancer. *J Exp Clin Cancer Res* **2012**, *31*, 68, doi:10.1186/1756-9966-31-68.
23. Dunne, P.D.; Dasgupta, S.; Blayney, J.K.; McArt, D.G.; Redmond, K.L.; Weir, J.A.; Bradley, C.A.; Sasazuki, T.; Shirasawa, S.; Wang, T.; et al. EphA2 Expression Is a Key Driver of Migration and Invasion and a Poor Prognostic Marker in Colorectal Cancer. *Clin Cancer Res* **2016**, *22*, 230-242, doi:10.1158/1078-0432.Ccr-15-0603.
24. Kamoun, W.S.; Kirpotin, D.B.; Huang, Z.R.; Tipparaju, S.K.; Noble, C.O.; Hayes, M.E.; Luus, L.; Koshkaryev, A.; Kim, J.; Olivier, K.; et al. Antitumour activity and tolerability of an EphA2-targeted nanotherapeutic in multiple mouse models. *Nat Biomed Eng* **2019**, *3*, 264-280, doi:10.1038/s41551-019-0385-4.
25. Jackson, D.; Gooya, J.; Mao, S.; Kinneer, K.; Xu, L.; Camara, M.; Fazenbaker, C.; Fleming, R.; Swamynathan, S.; Meyer, D.; et al. A human antibody-drug conjugate targeting EphA2 inhibits tumor growth in vivo. *Cancer Res* **2008**, *68*, 9367-9374, doi:10.1158/0008-5472.Can-08-1933.
26. Hasegawa, J.; Sue, M.; Yamato, M.; Ichikawa, J.; Ishida, S.; Shibutani, T.; Kitamura, M.; Wada, T.; Agatsuma, T. Novel anti-EPHA2 antibody, DS-8895a for cancer treatment. *Cancer Biol Ther* **2016**, *17*, 1158-1167, doi:10.1080/15384047.2016.1235663.
27. Annunziata, C.M.; Kohn, E.C.; LoRusso, P.; Houston, N.D.; Coleman, R.L.; Buzoianu, M.; Robbie, G.; Lechleider, R. Phase 1, open-label study of MEDI-547 in patients with relapsed or refractory solid tumors. *Invest New Drugs* **2013**, *31*, 77-84, doi:10.1007/s10637-012-9801-2.
28. Fraguas-Sánchez, A.I.; Lozza, I.; Torres-Suárez, A.I. Actively Targeted Nanomedicines in Breast Cancer: From Pre-Clinal Investigation to Clinic. *Cancers (Basel)* **2022**, *14*, doi:10.3390/cancers14051198.
29. Shitara, K.; Satoh, T.; Iwasa, S.; Yamaguchi, K.; Muro, K.; Komatsu, Y.; Nishina, T.; Esaki, T.; Hasegawa, J.; Kakurai, Y.; et al. Safety, tolerability, pharmacokinetics, and pharmacodynamics of the afucosylated,

 doi:10.20944/preprints202512.0860.v1

humanized anti-EPHA2 antibody DS-8895a: a first-in-human phase I dose escalation and dose expansion study in patients with advanced solid tumors. *J Immunother Cancer* **2019**, *7*, 219, doi:10.1186/s40425-019-0679-9.

30. Satofuka, H.; Suzuki, H.; Tanaka, T.; Li, G.; Kaneko, M.K.; Kato, Y. Development of an anti-human EphA2 monoclonal antibody Ea(2)Mab-7 for multiple applications. *Biochem Biophys Rep* **2025**, *42*, 101998, doi:10.1016/j.bbrep.2025.101998.
31. Ubukata, R.; Suzuki, H.; Hirose, M.; Satofuka, H.; Tanaka, T.; Kaneko, M.K.; Kato, Y. Establishment of a highly sensitive and specific anti-EphB2 monoclonal antibody (Eb2Mab-12) for flow cytometry. *Microbes & Immunity* **2025**, *0*, doi:10.36922/mi.5728.
32. Kaneko, M.K.; Suzuki, H.; Kato, Y. Establishment of a Novel Cancer-Specific Anti-HER2 Monoclonal Antibody H(2)Mab-250/H(2)CasMab-2 for Breast Cancers. *Monoclon Antib Immunodiagn Immunother* **2024**, *43*, 35-43, doi:10.1089/mab.2023.0033.
33. Kaneko, M.K.; Suzuki, H.; Ohishi, T.; Nakamura, T.; Tanaka, T.; Kato, Y. A Cancer-Specific Monoclonal Antibody against HER2 Exerts Antitumor Activities in Human Breast Cancer Xenograft Models. *Int J Mol Sci* **2024**, *25*, doi:10.3390/ijms25031941.
34. Kaneko, M.K.; Suzuki, H.; Ohishi, T.; Nakamura, T.; Yanaka, M.; Tanaka, T.; Kato, Y. Antitumor Activities of a Humanized Cancer-Specific Anti-HER2 Monoclonal Antibody, humH(2)Mab-250 in Human Breast Cancer Xenografts. *Int J Mol Sci* **2025**, *26*, doi:10.3390/ijms26031079.
35. Ubukata, R.; Ohishi, T.; Kaneko, M.K.; Suzuki, H.; Kato, Y. EphB2-Targeting Monoclonal Antibodies Exerted Antitumor Activities in Triple-Negative Breast Cancer and Lung Mesothelioma Xenograft Models. *Int J Mol Sci* **2025**, *26*, doi:10.3390/ijms26178302.
36. Suzuki, H.; Ohishi, T.; Tanaka, T.; Kaneko, M.K.; Kato, Y. Anti-HER2 Cancer-Specific mAb, H(2)Mab-250-hG(1), Possesses Higher Complement-Dependent Cytotoxicity than Trastuzumab. *Int J Mol Sci* **2024**, *25*, doi:10.3390/ijms25158386.
37. Satofuka, H.; Suzuki, H.; Tanaka, T.; Li, G.; Kaneko, M.K.; Kato, Y. Development of an anti-human EphA2 monoclonal antibody Ea2Mab-7 for multiple applications. *Biochemistry and Biophysics Reports* **2025**, *42*, doi:10.1016/j.bbrep.2025.101998.
38. Overdijk, M.B.; Verploegen, S.; Ortiz Buijsse, A.; Vink, T.; Leusen, J.H.; Bleeker, W.K.; Parren, P.W. Crosstalk between human IgG isotypes and murine effector cells. *J Immunol* **2012**, *189*, 3430-3438, doi:10.4049/jimmunol.1200356.
39. Pegram, M.; Hsu, S.; Lewis, G.; Pietras, R.; Beryt, M.; Sliwkowski, M.; Coombs, D.; Baly, D.; Kabbinavar, F.; Slamon, D. Inhibitory effects of combinations of HER-2/neu antibody and chemotherapeutic agents used for treatment of human breast cancers. *Oncogene* **1999**, *18*, 2241-2251, doi:10.1038/sj.onc.1202526.
40. Pietras, R.J.; Pegram, M.D.; Finn, R.S.; Maneval, D.A.; Slamon, D.J. Remission of human breast cancer xenografts on therapy with humanized monoclonal antibody to HER-2 receptor and DNA-reactive drugs. *Oncogene* **1998**, *17*, 2235-2249, doi:10.1038/sj.onc.1202132.
41. Baselga, J.; Norton, L.; Albanell, J.; Kim, Y.M.; Mendelsohn, J. Recombinant humanized anti-HER2 antibody (Herceptin) enhances the antitumor activity of paclitaxel and doxorubicin against HER2/neu overexpressing human breast cancer xenografts. *Cancer Res* **1998**, *58*, 2825-2831.
42. Gan, H.K.; Parakh, S.; Lee, F.T.; Tebbutt, N.C.; Ameratunga, M.; Lee, S.T.; O'Keefe, G.J.; Gong, S.J.; Vanrenen, C.; Caine, J.; et al. A phase 1 safety and bioimaging trial of antibody DS-8895a against EphA2 in patients with advanced or metastatic EphA2 positive cancers. *Invest New Drugs* **2022**, *40*, 747-755, doi:10.1007/s10637-022-01237-3.
43. Martini, G.; Cardone, C.; Vitiello, P.P.; Belli, V.; Napolitano, S.; Troiani, T.; Ciardiello, D.; Della Corte, C.M.; Morgillo, F.; Matrone, N.; et al. EPHA2 Is a Predictive Biomarker of Resistance and a Potential Therapeutic Target for Improving Antiepidermal Growth Factor Receptor Therapy in Colorectal Cancer. *Mol Cancer Ther* **2019**, *18*, 845-855, doi:10.1158/1535-7163.Mct-18-0539.
44. Markosyan, N.; Li, J.; Sun, Y.H.; Richman, L.P.; Lin, J.H.; Yan, F.; Quinones, L.; Sela, Y.; Yamazoe, T.; Gordon, N.; et al. Tumor cell-intrinsic EPHA2 suppresses anti-tumor immunity by regulating PTGS2 (COX-2). *J Clin Invest* **2019**, *129*, 3594-3609, doi:10.1172/jci127755.

 doi:10.20944/preprints202512.0860.v1

45. Shannon-Lowe, C.; Rickinson, A. The Global Landscape of EBV-Associated Tumors. *Front Oncol* **2019**, *9*, 713, doi:10.3389/fonc.2019.00713.
46. Young, L.S.; Yap, L.F.; Murray, P.G. Epstein-Barr virus: more than 50 years old and still providing surprises. *Nat Rev Cancer* **2016**, *16*, 789-802, doi:10.1038/nrc.2016.92.
47. Hu, H.; Luo, M.L.; Desmedt, C.; Nabavi, S.; Yadegarynia, S.; Hong, A.; Konstantinopoulos, P.A.; Gabrielson, E.; Hines-Boykin, R.; Pihan, G.; et al. Epstein-Barr Virus Infection of Mammary Epithelial Cells Promotes Malignant Transformation. *EBioMedicine* **2016**, *9*, 148-160, doi:10.1016/j.ebiom.2016.05.025.
48. Pathmanathan, R.; Prasad, U.; Sadler, R.; Flynn, K.; Raab-Traub, N. Clonal proliferations of cells infected with Epstein-Barr virus in preinvasive lesions related to nasopharyngeal carcinoma. *N Engl J Med* **1995**, *333*, 693-698, doi:10.1056/nejm199509143331103.
49. Hutt-Fletcher, L.M. Epstein-Barr virus entry. *J Virol* **2007**, *81*, 7825-7832, doi:10.1128/jvi.00445-07.
50. Chen, J.; Sathiyamoorthy, K.; Zhang, X.; Schaller, S.; Perez White, B.E.; Jardetzky, T.S.; Longnecker, R. Ephrin receptor A2 is a functional entry receptor for Epstein-Barr virus. *Nat Microbiol* **2018**, *3*, 172-180, doi:10.1038/s41564-017-0081-7.
51. Li, Y.; Zhang, H.; Sun, C.; Dong, X.D.; Xie, C.; Liu, Y.T.; Lin, R.B.; Kong, X.W.; Hu, Z.L.; Ma, X.Y.; et al. R9AP is a common receptor for EBV infection in epithelial cells and B cells. *Nature* **2025**, *644*, 205-213, doi:10.1038/s41586-025-09166-w.
52. Vo, D.N.K.; Ho, H.P.T.; Wu, L.S.; Chen, Y.Y.; Trinh, H.T.V.; Lin, T.Y.; Lim, Y.Y.; Tsai, K.C.; Tsai, M.H. Broad-spectrum antiviral activity of Ganoderma microsporum immunomodulatory protein: Targeting glycoprotein gB to inhibit EBV and HSV-1 infections via viral fusion blockage. *Int J Biol Macromol* **2025**, *307*, 142179, doi:10.1016/j.ijbiomac.2025.142179.
53. Hosking, M.P.; Shirinbak, S.; Omilusik, K.; Chandra, S.; Kaneko, M.K.; Gentile, A.; Yamamoto, S.; Shrestha, B.; Grant, J.; Boyett, M.; et al. Preferential tumor targeting of HER2 by iPSC-derived CAR T cells engineered to overcome multiple barriers to solid tumor efficacy. *Cell Stem Cell* **2025**, *32*, 1087-1101.e1084, doi:10.1016/j.stem.2025.05.007.